Environmental Science & Technology

pubs.acs.org/est

Article

Rapid Simulation of Decade-Scale Charcoal Aging in Soil: Changes in Physicochemical Properties and Their Environmental Implications

Xiao Chen, Xiaodong Gao, Pingfeng Yu, Leonardo Spanu, Jessica Hinojosa, Shuqi Zhang, Mingce Long, Pedro J. J. Alvarez, and Caroline A. Masiello*

Cite This: *Environ. Sci. Technol.* 2023, 57, 128−138

Read Online

ACCESS | Metrics & More | Article Recommendations | Supporting Information

ABSTRACT: *In situ* aging can change biochar properties, influencing their ecosystem benefits or risks over time. However, there is a lack of field verification of laboratory methods that attempt simulation of long-term natural aging of biochar. We exploited a decade-scale natural charcoal (a proxy for biochar) aging event to determine which lab-aging methods best mimicked field aging. We oxidized charcoal by ultraviolet A radiation (UVA), H_2O_2, or monochloramine (NH_2Cl), and compared it to 10-year field-aged charcoal. We considered seven selected charcoal properties related to surface chemistry and organic matter release, and found that oxidation with 30% H_2O_2 most representatively simulated 10-year field aging for six out of seven properties. UVA aging failed to approximate oxidation levels while showing a distinctive dissolved organic carbon (DOC) release pattern. NH_2Cl-aged charcoal was the most different, showing an increased persistent free radical (PFR) concentration and lower hydrophilicity. All lab oxidation techniques overpredicted polycyclic aromatic hydrocarbon release. The O/C ratio was well-correlated with DOC release, PFR concentration, surface charge, and charcoal pH, indicating the possibility to accurately predict biochar aging with a reduced suite of physicochemical properties. Overall, our rapid and verified lab-aging methods facilitate research toward derisking and enhancing long-term benefits of biochar application.

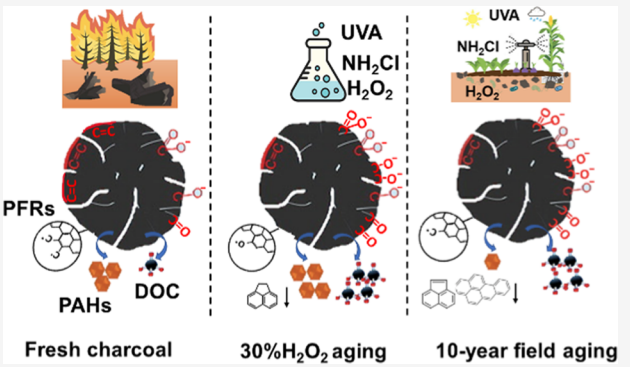

KEYWORDS: *char, aging, simulation, dissolved organic carbon, polycyclic aromatic hydrocarbons, persistent free radicals, surface charge, contact angle*

INTRODUCTION

Production of biochar and its application in soil have been proposed to improve soil fertility and hydrology,[1] remove Gt-scale amounts of atmospheric CO_2,[2] facilitate production of carbon-negative bioenergy,[3,4] and remediate contaminated soil and water.[5] While biochar persists in the environment, its ecosystem services may change with time because the physicochemical properties that deliver these services evolve on the timescale of years to decades. Therefore, understanding system-specific risks and benefits of biochar application requires long-term monitoring, which represents a logistical challenge.

We currently lack field verification of laboratory biochar aging methods, which is necessary to assess the long-term environmental behavior of commercial biochar.[6−8] Various laboratory methods have been proposed to simulate and accelerate the processes that occur during biochar natural aging. Most approaches have focused on short-term (<1.5 years) changes in biochar surface chemistry via aging by (photo)chemical (e.g., HNO_3/H_2SO_4,[9] NaClO, H_2O_2,[10] sunlight[11,12]), biological (e.g., microbial inoculum extracted from soil[13−15] or organic exudates of plant roots[16]), and physical methods (e.g., high temperature, freeze−thaw cycles,[14] wet−dry cycles[17]). Other previous work includes using lab incubations to predict 100-year mineralization of biochar in soils,[18] and comparison of leached polycyclic aromatic hydrocarbon (PAH) concentration and composition between lab-aged and 4-year field-aged biochar.[19] However, none of these previous studies were validated by directly comparing lab-oxidized biochar to long-term naturally aged biochar in terms of both surface chemistry and organic matter release. We postulate that charcoal can be used as a biochar proxy due to their chemical similarity.[6] Here, we used a decade-long natural charcoal aging to validate different lab-aging methods with respect to a suite of charcoal properties. We aimed to find out which simulated weathering approach could accurately mimic long-term natural processes.

Received: July 18, 2022
Revised: December 4, 2022
Accepted: December 6, 2022
Published: December 16, 2022

https://doi.org/10.1021/acs.est.2c04751
Environ. Sci. Technol. 2023, 57, 128−138

We artificially aged the "fresh" charcoal by designing aging techniques to simulate a range of potential environmental exposures: ultraviolet A (UVA) oxidation to simulate UV-driven reactions likely to occur in surface soils and natural waters; H_2O_2 (which can be released by soil biota[20−22]) oxidation to simulate natural, long-term environmental microbial oxidation; and monochloramine (NH_2Cl) oxidation (NH_2Cl is a common residual disinfectant) to simulate reactions that could occur when soil charcoal is exposed to tap water or reclaimed wastewater.[23,24]

We compared lab-aged charcoal oxidized by UVA, H_2O_2, and NH_2Cl to the 10-year field-aged charcoal from the same site after weathering *in situ* with respect to a suite of carefully chosen properties. First, O/C ratio and surface oxygen-containing functional groups reflect the oxidation level of char and may influence other properties measured in our study.[25−27] Second, we measured extractable dissolved organic carbon (DOC) yield because (1) DOC concentration is a general screen for the release of carbon-containing compounds (e.g., PAHs) from char,[28,29] and (2) DOC is a general marker for the potential impact of a carbonaceous material on the ecosystem food web structure, given its effects on the light availability to photosynthesizers and as a food source for decomposers.[30] Third, persistent free radicals (PFRs) have been found in pyrogenic carbon (e.g., biochar) with half-lives ranging from a few hours to several days.[31−34] PFRs can trigger the formation of reactive oxygen species (ROS), such as hydroxyl radicals ($^{\bullet}OH$). This could damage soil microorganisms, inhibit plant growth,[35] or affect other ecosystem functions (e.g., dissolved organic matter transformation)[36] even at low PFR concentrations. Only limited information is available on PFRs in wildfire-derived charcoal to date.[27] Fourth, we measured zeta potential (ζ), the electric potential at the hydrodynamic slipping plane, which is related to a particle's surface charge[37,38] and can be used as a proxy for the nutrient sorption characteristics. Fifth, we measured contact angle because it can be used to assess charcoal wettability,[39] which affects soil hydraulic properties (i.e., runoff/infiltration ratio). Finally, we measured 16 USEPA priority PAHs, due to their carcinogenic, teratogenic, and mutagenic potential.[40,41] Here, we report a rapid and validated lab-aging approach for the semiquantitative simulation of long-term biochar aging effects.

MATERIALS AND METHODS

Charcoal. Fresh charcoal was immediately collected from the remains of an East Texas forest burned entirely to the ground during the 2011 U.S. drought[42] and stored dark and dry in our lab for 10 years. Although char may gradually oxidize during storage,[43] especially if exposed to moist air and/or reactive oxygen species, our lab-stored "fresh charcoal" was indistinguishable in the oxidation level reflected by the O/C ratio (0.12 ± 0.04) (Figure 2 and Table S2) compared to the reported O/C ratio of fresh charcoal (0.10−0.19).[25,44] We resampled soil charcoal 10 years later in 2021 from the same location (Text S1), creating a controlled before−after environmental aging experiment under hot, humid climate conditions known to drive rapid charcoal oxidation.[25] This site experiences more extreme weathering conditions with mean annual temperature 4 °C higher than extremes reported by previous biochar natural weathering studies.[25,45] Both fresh and field-aged charcoal were ground and sieved to 0.250−0.853 mm. Here, we use "charcoal" to mean natural charcoal and "char" to mean both biochar and charcoal.

Charcoal Aging. *UVA Aging.* UVA is the main component of UV light in the solar spectrum, making up 4−5% of the total solar irradiation. The intensity of UVA reaching the ground is relative to altitude, seasonal variation, and weather conditions,[46,47] ranging up to 7 mW cm^{-2}.[48−50] Specifically, the UVA intensity in Houston, TX, was approximately between 1 and 5 mW cm^{-2} measured at the ground level on a winter day, depending on the weather conditions. In our study, the light intensity at the center of the reactor was measured at 0.8 mW cm^{-2} using a radiometer (UVA/B light meter 850009, SPER SCIENTIFIC), which was the maximum light intensity generated by this photoreactor. To compensate the relatively low output of this photoreactor, we ran experiments continuously for 10 days.[50,51]

We performed irradiation experiments in a custom photoreactor.[52] The photoreactor was equipped with six 4 W black lamps (EIKO F4T5/BLB) that emitted UVA in the wavelength range of 300−400 nm centered at 350 nm. In each experiment, one 200 mL Pyrex glass beaker (covered with a glass Petri dish) contained 5 g of charcoal and 100 mL of DI water,[53] which was placed on the magnetic stirrer at the center of the photoreactor. Water was adjusted in the beaker every 24 h due to evaporative loss. We withdrew samples from the beaker for analysis at days 0, 1, 3, 7, and 10, and then filtered through a 0.3 μm glass fiber filter (Advantec, GF-75, preheated at 500 °C for 6 h).[54,55] The filtrate was collected for DOC analysis using a Shimadzu TOC-VCSH analyzer (Text S2). The aged charcoal was collected at day 10, washed with 300 mL of DI water, and then dried in an oven at 60 °C overnight for further characterization. We conducted dark control experiments in a similar way but with the beaker wrapped with aluminum foil. Our blank control was identical to the dark control but without charcoal. In addition, we also employed sterilization and natural water to explore DOC loss in the charcoal dark control experiment (Text S3).

H_2O_2 Aging. H_2O_2 can be released into the soil environment by microbes to oxidize biochar.[56−58] For example, the bacterium *Lactobacillus johnsonii* NCC 533 can excrete up to 0.003% H_2O_2 within 10 h.[59] Different H_2O_2 concentrations have been used for other accelerated aging experiments, ranging from 5 to 30% H_2O_2 for 2 h−4 months either at room temperature or with heat treatment.[56,60−66] The higher H_2O_2 concentration resulted in a higher biochar oxidation extent under the same exposure duration.[66] We selected the high and low end of the reported H_2O_2 concentrations but with some alteration to the duration and temperature: 30% H_2O_2 (180 min)[66] and 5% H_2O_2 (48 h)[61] at room temperature. We aimed to develop a rapid and facile lab-aging approach that agrees with the results of our field aging experiencing more extreme weathering conditions.[25,45]

Briefly, 5 g of charcoal was placed into a glass bottle containing 100 mL of H_2O_2 (30 or 5%). Then, the capped glass bottle was shaken for 180 min (30%) and 48 h (5%), respectively. An aliquot was withdrawn from the glass bottle at a designated time and then went through the same processes as UVA aging for analyses of filtrate and aged charcoal. Controls included the mixture of 5 g charcoal in 100 mL of DI water and just 100 mL of H_2O_2 (30 or 5%).

NH_2Cl Aging. NH_2Cl is a common drinking water disinfectant. NH_2Cl has also been used as an alternative to chlorine during wastewater treatment processes, for example, to mitigate biofouling in transport pipes, where the residual NH_2Cl is ∼1 mg L^{-1}.[23] The USEPA has set the maximum

https://doi.org/10.1021/acs.est.2c04751
Environ. Sci. Technol. 2023, 57, 128−138

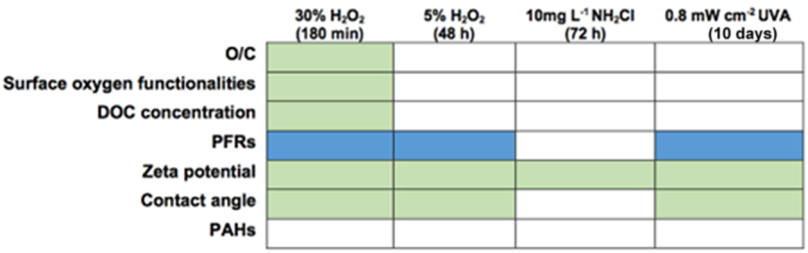

Figure 1. Performance of accelerated lab-aging methods in simulating field aging. Different colors represent how lab aging mimicked field aging with different statistical significances. White: lab aging was unable to mimic field aging ($p < 0.05$). Green: lab aging was able to simulate field aging ($p > 0.05$). Blue: lab aging was able to mimic field aging just for PFR concentration rather than PFR types ($p > 0.05$). The p value for each property of each lab-aged charcoal as compared to that of field-aged charcoal was shown in Table S1.

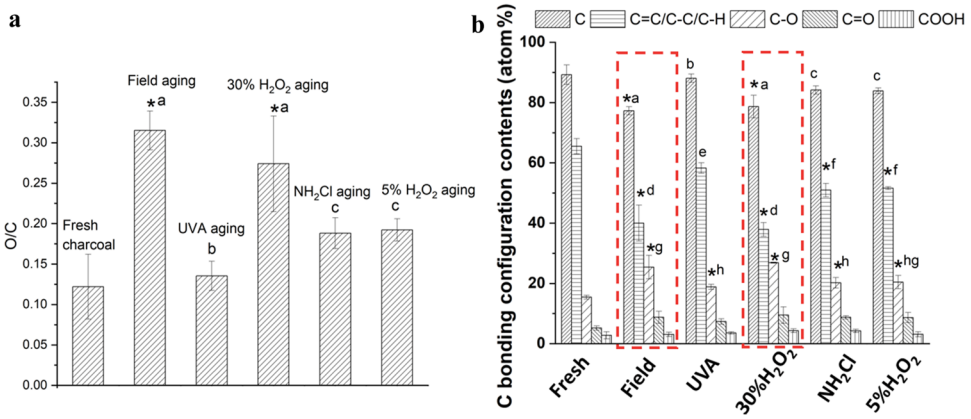

Figure 2. (a) O/C ratios and (b) C bonding configuration contents of charcoal before and after aging. Error bars represent ± one standard deviation from the mean of triplicate treatments. Asterisks (*) indicate significant oxidation of the aged charcoal compared to fresh charcoal ($p < 0.05$). For each bonding configuration, columns with different letters between lab- and field-aged samples represent statistically significant differences ($p < 0.05$) in the content of this specific bonding configuration between lab- and field-aged samples.

residual disinfectant level for chloramines (measured as Cl_2) at 4.0 mg L^{-1},[24] which gave us an approximate bound for experimental NH_2Cl oxidation values. To the best of our knowledge, there is limited research about biochar aging by NH_2Cl, although other researchers have used other chlorine species (e.g., NaClO).[10] In our study, NH_2Cl concentration was set at 10 mg L^{-1} (72 h) to accelerate charcoal aging.[67−70]

We prepared fresh NH_2Cl stock solutions daily using NaClO solution and NH_4Cl solution (Text S4), using a diluted working solution of 10 mg L^{-1} NH_2Cl. Specifically, 5 g of charcoal was placed into a glass bottle containing 100 mL of 10 mg L^{-1} NH_2Cl and 10 mM phosphate-buffered solution (PBS) (pH = 7). Then, the capped glass bottle was shaken for 72 h. Collection and analyses of filtrate and aged charcoal were the same as UVA and H_2O_2 aging. Controls included the mixture of 5 g of charcoal in 100 mL of DI water and just 100 mL of 10 mg L^{-1} NH_2Cl solution containing 10 mM PBS.

DOC Leaching Experiments. We used the same procedure adopted for the charcoal dark control in DI water in the UVA-aging section. As before, we agitated 5 g of charcoal before or after aging to 100 mL of DI water on a shaker for 10 days under dark conditions, and then sampled at the same designated time to see which lab-aging method best mimicked field aging in terms of DOC yield.

Charcoal Characterization. Charcoal characterization included X-ray photoelectron spectroscopy (XPS) for O/C ratio and surface oxygen-containing functional groups, attenuated total reflectance Fourier transform infrared spectroscopy (ATR-FTIR), ζ potential, contact angle, PFR analyses, charcoal pH, surface area, and pore volume (details provided in Text S5).

PAH Analysis. Accelerated solvent extraction (DIONEX ASE 350) was used to extract PAHs from fresh, lab-aged, and field-aged charcoal with dichloromethane (DCM)/acetone (ACE) (1:1, v/v) as extraction solvent[40] (Text S6).

PAHs in the charcoal ASE extract were measured on a Shimadzu FRC-10A HPLC system (Text S7). EPA 610 mixture standard was diluted to different concentrations in DCM/ACE (1:1, v/v) for calibration curves.

Statistical Analysis. All of the experiments in our study were done in triplicate. We used a two-tailed Student's t-test to determine whether the differences between the untreated samples and the aged samples were significant at the 95% confidence level. A one-way analysis of variance (ANOVA) with a post hoc t-test was used to determine the statistical significances between the aged samples.

RESULTS AND DISCUSSION

Although there are many other potential properties that can be measured, we argue that this suite of seven measurements we chose here, which were closely associated with environmental benefits and risks, provided an overview screen for understanding the potential environmental effects of biochar soil amendments. The overall findings are summarized in Figure 1.

O/C Ratio and Surface Oxygenation. Oxidation of charcoal is generally initiated on the surface of particles[44,71] and remains close to the surface even with several hundred years of exposure in soil.[72] We used XPS (with a maximum

https://doi.org/10.1021/acs.est.2c04751
Environ. Sci. Technol. 2023, 57, 128−138

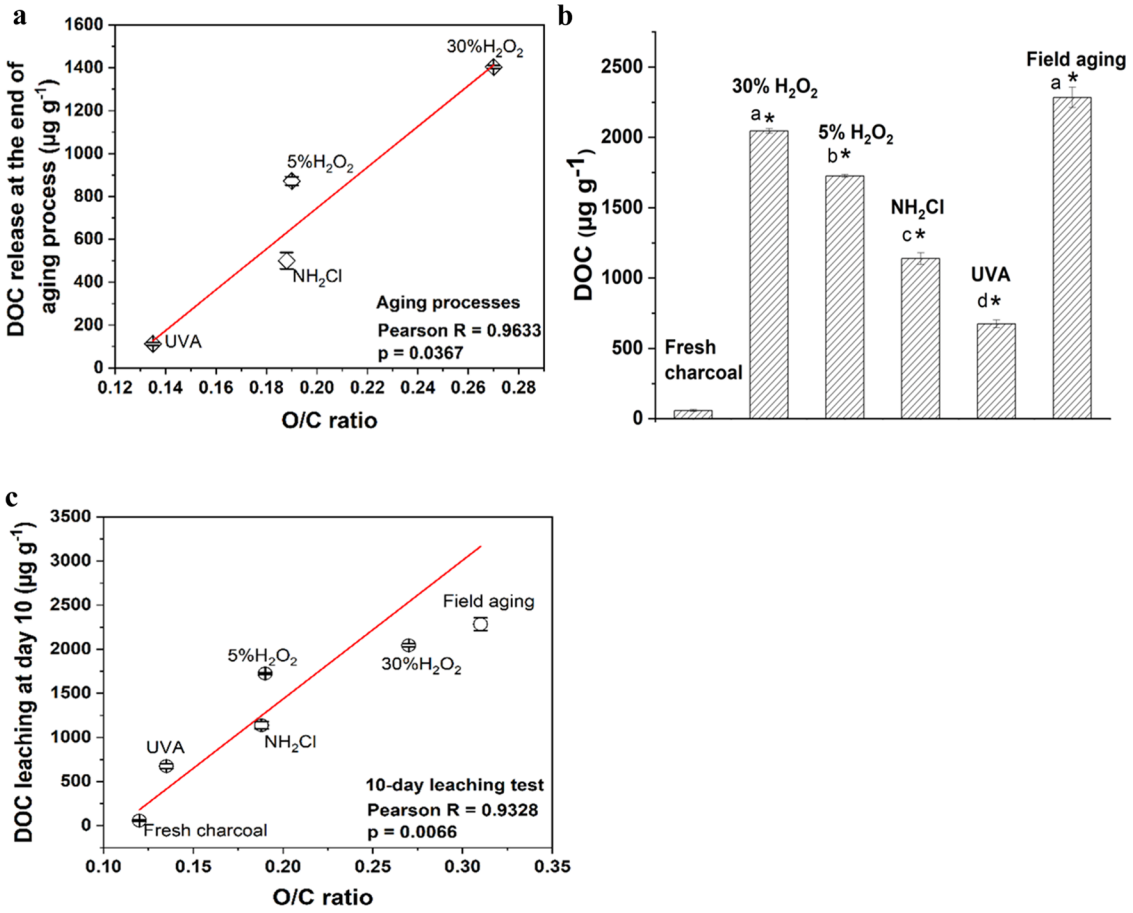

Figure 3. (a) Relationship between O/C ratios of charcoal and their DOC release at the end of each aging process. (b) Comparison between DOC yield at day 10 from fresh, lab-aged, and field-aged charcoal. (c) Relationship between O/C ratios of charcoal and their DOC release at day 10 during the 10-day leaching test. Error bars represent ± one standard deviation from the mean of triplicate treatments. Asterisks (*) indicate statistically significant differences between aged charcoal and fresh charcoal ($p < 0.05$). Columns with different letters represent statistically significant differences ($p < 0.05$) between lab- and field-aged samples.

penetration depth of ~10 nm[44]) to explore changes in the O/C ratio and ingrowth of oxygen functional groups caused by charcoal oxidation.

Oxidation Level Changes. We explored how both field and lab aging affected the oxidation level of char, indicated by the O/C ratio and surface oxygen functionalities. Both UVA intensity/oxidant concentration and aging duration collectively affected the extent of char oxidation. Among all of the lab-aging methods, 30% H_2O_2 (180 min) aging most oxidized fresh charcoal to the highest O/C ratio (0.27 ± 0.06), while UVA aging (0.8 mW cm^{-2}, 10 days) tended to exhibit the lowest oxidation capability. There was no statistically significant difference in the O/C ratio between 5% H_2O_2 (48 h) and NH_2Cl aging (10 mg L^{-1}, 72 h) (Figure 2a and Table S2). The oxidation level of the 10-year field-aged charcoal was on the high end of the aged charcoal. The O/C ratio (0.29 ± 0.02) of the 10-year field-aged charcoal had no statistically significant difference from that of 30% H_2O_2-aged charcoal. The observed O/C ratios fell into the reported O/C range for UVA-, H_2O_2-, or field-aged char (0.13−0.45).[11,27,56,62,64] The results implied the dissolution of labile C[73] and C mineralization[74] during lab aging. The increases in O in our study were associated with the formation of surface oxygen-containing functionalities as observed by XPS (see discussion below).

We also considered changes in C and O bonding configurations after charcoal aging. Common bonding configuration types of C can be found via XPS, including C═C/C−C/C−H (284.70 ± 0.11 eV), C−O (286.19 ± 0.28 eV), carbonyl (C═O) (288.29 ± 0.51 eV), and carboxyl (COOH) groups (290.41 ± 0.82 eV) (Figure S1 and Table S2),[11,25,44,75,76] which was also evidenced by FTIR analysis (Figure S2). The contents of C═C/C−C/C−H in all of the aged charcoal tended to decline following treatment compared with fresh charcoal (Figure 2b). Conversely, all of the aged charcoal had an increase in the contents of surface oxygen functionalities (especially the C−O group). These results were similar to previous research showing that UVA, H_2O_2, and field aging introduced more oxygen functionalities (e.g., phenolic (OH), C═O, and COOH groups) onto char surfaces over time.[7] Among all of the lab-aged charcoal, 30% H_2O_2-aged charcoal had the lowest C═C/C−C/C−H (37.99 ± 3.61 atom %) and highest C−O contents (26.95 ± 1.41 atom %), while UVA-aged charcoal tended to exhibit the highest C═C/C−C/C−H albeit with a lower C−O content. There was no statistically significant difference between C bonding configuration contents of 5% H_2O_2 and NH_2Cl-aged charcoal, which was consistent with the changes in the composition of O bonding configurations of the lab-aged charcoal (Figure S1n). The trend in the O/C ratio along with surface oxygen-containing functional groups in the lab-aged charcoal suggests

https://doi.org/10.1021/acs.est.2c04751
Environ. Sci. Technol. 2023, 57, 128−138

that charcoal underwent photooxidation or chemical oxidation reactions with the possible oxidative contribution from the generated ROS (e.g., $^{\bullet}OH$, singlet oxygen ($^1O_2$), or superoxide radical ($O_2^{\bullet-}$)[56]) in the aging systems. The 10-year field-aged charcoal had the highest contents of surface oxygen functionalities (especially C−O: 25.40 ± 3.46 atom %) without a statistically significant difference from that of 30% H_2O_2-aged charcoal, which indicated the occurrence of abiotic and biotic oxidation reactions during natural aging as well as adsorption of noncharcoal substances (e.g., humic acid).[76−78]

Simulation Performance. To explore which lab-aging method best simulated natural aging in terms of oxidation level, we compared both O/C ratios and contents of surface oxygen-containing bonding configurations between lab- and field-aged charcoal. 30% H_2O_2-aged charcoal (O/C: 0.27 ± 0.06, C−O: 26.95 ± 1.41 atom %) was the most oxidized among all of the lab-aged charcoal ($p < 0.05$) and produced a XPS profile closest to that of field-aged charcoal.

Overall, increasing the H_2O_2 dose to 180 min of aging in 30% H_2O_2 significantly enhanced the oxidation level of fresh charcoal to more closely match with that of the field-aged charcoal. UVA aging tended to induce the lowest oxidation level to fresh charcoal. There was no statistically significant difference in the oxidation levels between 5% H_2O_2 and NH_2Cl aging.

DOC Release. *Lab Aging.* Lab aging of charcoal caused significant changes to the released DOC flux (Figure S3a−d). H_2O_2 and NH_2Cl aging increased DOC flux. The released DOC increased with the H_2O_2 dose with 70.2 mg L^{-1} (1,404 μg DOC g^{-1} charcoal) for 30% H_2O_2 (180 min) (Figure S3a) and 43.6 mg L^{-1} (872 μg DOC g^{-1} charcoal) for 5% H_2O_2 (48 h) (Figure S3b). NH_2Cl treatment for 72 h led to a lower DOC release of 25.0 mg L^{-1} (500 μg DOC g^{-1} charcoal) (Figure S3c). However, 10-day UVA aging decreased the DOC flux from 12.9 mg L^{-1} (258 μg DOC g^{-1} charcoal) to 5.6 mg L^{-1} (112 μg DOC g^{-1} charcoal), which corresponded to 56% DOC mineralization (Figure S3d). This might be due to the production of DOC-generated ROS including $^1O_2$ and $O_2^{\bullet-}$ in the UVA-aging system.[51] We additionally observed that DOC release in the charcoal dark control experiment in DI water increased till day 1, then sharply decreased (by 77% at day 10) (Figure S3d), which was associated more with re-adsorption of DOC onto charcoal than microbial degradation (for a detailed explanation see Figure S4). DOC release during the aging processes tended to positively correlate with the O/C ratios of charcoal (Pearson $R = 0.9633$, $p = 0.0367$, Figure 3a). The greater functionalization of the condensed aromatic clusters in char as its oxidation level increased tended to increase aqueous solubility of char.[79]

Leaching Experiment. Either lab or field aging increased DOC 10-day leaching compared with that of fresh charcoal (Figures 3b and S3e). The DOC release was between 674 and 2284 μg DOC g^{-1} at day 10. 30% H_2O_2-aged charcoal had the greatest DOC release of 2045 ± 17 μg DOC g^{-1} charcoal among lab-aged charcoal (Figure 3b). However, there was a sharp decrease (by ∼70%) in DOC release during UVA-aged charcoal leaching at day 7 (Figure S3e), which might be associated with the re-sorption of the released DOC to the UVA-aged charcoal due to change in its morphology and porosity (with a higher surface area and mesopore volume among lab-aged charcoal, Table S3).[80] DOC release from field-aged charcoal was at the high end among all of the aged charcoal, which could stem from both the intrinsic DOC of charcoal and DOC adsorbed from the surrounding environment with aromatic DOC fraction being preferentially sorbed.[81] There was no statistically significant difference in DOC released at day 10 between 30% H_2O_2-aged charcoal and field-aged charcoal (Figure 3b). DOC release during the 10-day leaching test also tended to positively correlate with the O/C ratios of charcoal (Pearson $R = 0.9328$, $p = 0.0066$, Figure 3c). The positive relationship between O/C ratios and DOC release of charcoal could be because the higher content of surface negative charges in the more oxidized aged charcoal (see discussion below in Figures 4b and S5c) can repel more of the dissociated DOC fractions.[82]

Simulation Performance. DOC flux increased with the oxidation level suggests that char aging in soil could facilitate translocation of solutes to the aqueous system.[83−85] The range of DOC concentrations observed here fell within the reported ones of DOC release from pyrogenic carbon (48.2−13,700 μg DOC g^{-1} biochar[51,53,73,86]). However, this screen alone is not enough to draw definitive conclusions about the impacts of this material on ecosystem processes (explanation seen in Figure S3), which deserves further attention.

Overall, the aged charcoal with a higher oxidation level tended to release more DOC. UVA aging induced a distinctive pattern of DOC release: (1) DOC flux decreased during the aging process; and (2) DOC release increased and then dwindled over time during the 10-day leaching test of UVA-aged charcoal. 30% H_2O_2 aging could mimic field aging best with respect to DOC release during 10-day leaching.

Surface Chemistry. *Persistent Free Radicals.* Electron paramagnetic resonance (EPR) can be used to detect PFRs in materials with aromatic functional groups like charcoal. We used the overall peak height to approximate the total amount of PFRs and the *g* factor of EPR curves (representing the PFR paramagnetic center's electronic structure and therefore PFRs' neighboring chemical structures[87,88]) to characterize PFR present (Figure S5a). Fresh and field-aged charcoal contained carbon-centered PFRs, as indicated by their *g*-factor values < 2.0030, but lab-aged charcoal had higher *g* factors (Figures 4a and S5a) indicating oxygenated carbon-centered PFRs.[89] 30% H_2O_2, 5% H_2O_2, UVA, and field aging tended to decrease the PFR concentration in fresh charcoal albeit with no statistically significant difference, whereas NH_2Cl aging increased the PFR concentration (Figure 4a). This implies the potential reactions between charcoal and chlorinated waters and needs further exploration. With that being said, the aged charcoal with a higher oxidation level tended to have a lower PFR concentration (Pearson $R = -0.9885$, $p = 0.0115$, excluding NH_2Cl and UVA aging, Figure S5b). These results coincided with previous research documenting (1) a negative relationship between PFR abundance and molar O/C ratio, which is because a higher oxidation level might reduce the size of aromatic clusters therefore influence the stability of PFRs;[89] and (2) a decrease observed by other researchers in charcoal's PFR concentration after 5-year field aging.[27] Overall, 30% H_2O_2, 5% H_2O_2, and UVA aging can mimic field aging in terms of PFR concentration but failed with respect to PFR types.

PFR trends observed here may help to explain other data sets in our study. PFRs could be one of the sources of ROS in our charcoal aging experiments given the possible interaction of PFRs with water,[90,91] O_2, or H_2O_2.[35,92] The formation of those ROS may not only affect the DOC degradation/release from the aging experiments (Figure S3a−d) but also may

https://doi.org/10.1021/acs.est.2c04751
Environ. Sci. Technol. 2023, 57, 128−138

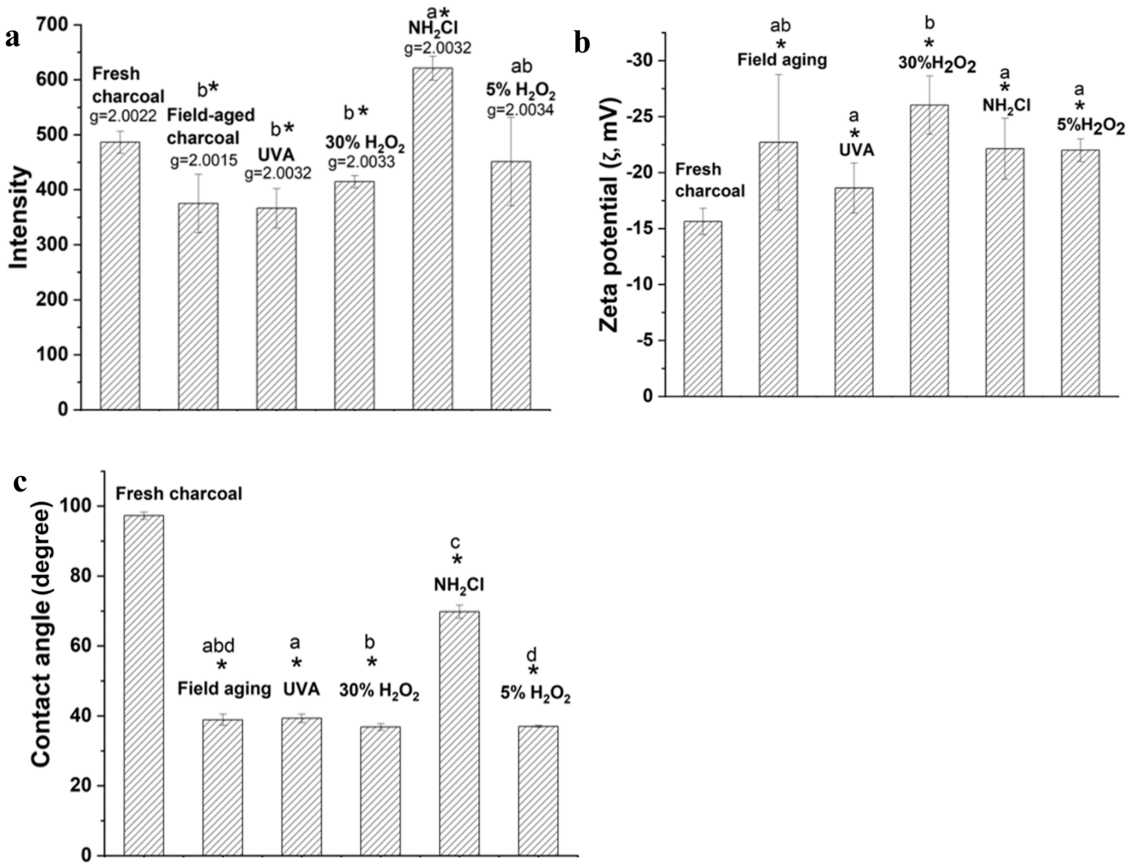

Figure 4. (a) Type and concentration of persistent free radicals (g = g factor), (b) zeta potential (ζ, pH = 7, T = 25 °C), and (c) contact angle detected in fresh, lab-aged, and field-aged charcoal. Asterisks (*) indicate significant changes in surface chemistry of the lab-aged and field-aged charcoal compared to fresh charcoal. Columns with different letters represent statistically significant differences ($p < 0.05$) between lab- and field-aged samples. Error bars represent ± one standard deviation from the mean of triplicate treatments.

contribute to the oxidation of the solid charcoal matrix.[56] Furthermore, the decrease in the PFR concentration after aging may reduce the potential risks posed by the PFR-derived ROS.

Surface Charge. The negative ζ (pH = 7, 25 °C) of all of the charcoal (Figure 4b) indicated negative surface charges.[37] All of the aged charcoal had more negative surface charge than fresh charcoal, consistent with previous studies of both artificial and field aging of char.[25,93] Overall, there was no statistically significant difference in ζ between all of the lab-aged charcoal and field-aged charcoal. The three types of lab-aging methods considered here approximated field aging in terms of ζ.

We found a positive relationship between the O/C ratio and charcoal ζ (absolute value), except for field-aged charcoal (Pearson R = 0.9715, p = 0.0058, Figure S5c). This is because the more oxidized aged charcoal tended to have more surface oxygen functionalities (Figure 2). The negative charge on charcoal surfaces stems primarily from the dissociated surface oxygen-containing functionalities (e.g., COOH and OH groups).[82] The exception of field-aged charcoal to the positive relation between the O/C ratio and ζ might be associated with a surface positive charge formed due to soil mineral weathering, especially in tropical soils.[94] Enhanced negative surface charge after aging may increase the cation exchange capacity,[37,44,95] which is conducive to the enhanced soil fertility.[96,97]

Contact Angle. Fresh charcoal was slightly hydrophobic, with a contact angle > 90°,[98] but all of the aged charcoal had contact angles lower than 90° (Figure 4c). However, we observed no statistically significant difference between contact angles of UVA-, 30% H_2O_2-, or 5% H_2O_2-aged and that of field-aged charcoal. The hydrophilicity of biochar was collectively affected by and positively correlated with surface oxygen functionalities (especially COOH), surface area, and mesopore volume.[99] Although UVA- and 5% H_2O_2-aged charcoal had the lower oxidation level (Figure 2), they tended to have a higher surface area and mesopore volume (Table S3) but no significant difference in the COOH content (Figure 2b) compared with the 30% H_2O_2-aged charcoal, which could account for the absence of relationship between O/C ratio and charcoal hydrophilicity. The relatively higher contact angle of NH_2Cl-aged charcoal might be additionally associated with formation of C−Cl bound on its surface.[67,68,100] Overall, all of the lab-aging methods enhanced the hydrophilicity of charcoal, and all methods except NH_2Cl aging can approximate field aging in terms of contact angle.

Notably, the wettability alone does not control the hydrologic impacts of chars, which is driven holistically by a suite of properties including the grain size of the char relative to the amended soil, the internal porosity of the char itself,[101] and the wettability of soil itself and its total organic carbon content.[99]

PAH Release Trends. No laboratory-aging method was able to reproduce natural field aging with respect to PAH release trends. Field aging of charcoal samples significantly decreased the amount of PAHs released, while laboratory aging

https://doi.org/10.1021/acs.est.2c04751
Environ. Sci. Technol. 2023, 57, 128−138

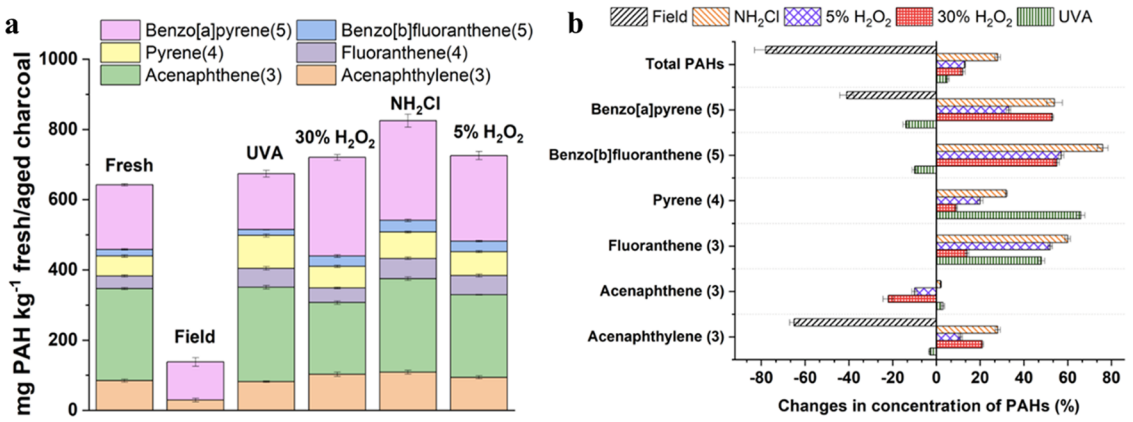

Figure 5. (a) PAH concentration (subtracting peak area of ASE control) and composition in fresh and aged charcoal. (b) PAH concentration change (%) in each aged charcoal. Number in parentheses was the ring number of each of PAHs. Error bars represent ± one standard deviation from the mean of triplicate treatments.

typically increased it. The total PAHs potentially existing in fresh, lab-aged, and field-aged charcoal were 643, 674−825, and 138 mg kg^{-1} (Figures 5a and S6, Tables S4 and S5), respectively, which fell into the range of the total concentrations of 16 USEPA priority PAHs reported for 43 biochar samples produced at 400−750 °C (ranging from 0.4 to 2000 mg kg^{-1}).[102] These results exceeded the limit value set by the European Biochar Certificate for basic-grade (<30 mg kg^{-1}) and premium-grade (<4 mg kg^{-1}) biochar.[103] Acenaphthylene, acenaphthene, fluoranthene, pyrene, benzo[*b*]fluoranthene, and benzo[*a*]pyrene with three−five rings were the most abundant PAHs in the fresh and lab-aged charcoal.

The changes in the total concentration and composition of PAHs extracted from fresh and aged charcoal depended on the aging methods and pyrogenic carbon type. UVA aging did not significantly change overall PAH concentration (5%) but showed a trend of increasing (3−66%) three- and four-ring PAHs (with exception to a slight decrease (−3%) in three-ring acenaphthylene) and decreasing five-ring PAHs (−14 to −10%). On the other hand, H_2O_2- and NH_2Cl-aged charcoal presented an increasing trend for both overall (12−28%) and individual three−five ring PAH (7−76%) concentration (with exception to a decrease in three-ring acenaphthene in 30% and 5% H_2O_2 aging, of −22 and −10%, respectively) (Figure 5b and Table S5). This observation coincided with previous research.[104] The observed increase in the PAHs released (especially with three and four rings) might be because of the altered morphology of charcoal after all three lab-aging methods facilitated the extraction of PAHs, which would otherwise be encapsulated in charcoal before aging.[105] Alternatively, the increase in PAH release might be relative to the possible PAH formation during laboratory aging including (1) ring addition to a molecule of PAHs through an acetylene addition mechanism under UV irradiation,[106] and (2) the reaction between $^{\bullet}OH$ generated during aging and arrays of sp^2 carbon in char.[107] On the other hand, $^{\bullet}OH$ may also contribute to PAH loss through conversion of PAHs to alcohols or ketones.[108]

In contrast, the total PAH content of charcoal decreased significantly after field aging, which was consistent with previous research.[19] The field-aged charcoal also had a lower diversity in PAH types with only acenaphthylene and benzo[*a*]pyrene as the possible major PAHs. All laboratory-aging methods tested here failed to accurately replicate natural PAH release, which might relate to the absence of mixing charcoal with soil in the artificial aging approaches. Charcoal aging could affect the release of native soil PAHs from soil organic matter (SOM, i.e., humic substances) through changing the extractable-SOM/stable-SOM ratio, soil particle size, and charcoal affinity toward PAHs (Table S5),[109] which involves mechanisms including physisorption,[110] microbial uptake and degradation, leaching, photochemical oxidation, and transportation to mineral phase.[111] Explanations for the failure of laboratory aging to match field aging in PAH release may provide information about the potential limitations of various lab-aging techniques. However, the risk of PAH release decreases as charcoal ages compared with fresh charcoal. The value of 138 mg PAHs kg^{-1} for field-aged charcoal was within the maximum allowable threshold of 300 mg kg^{-1} set by the International Biochar Initiative.[112]

Our work confirmed the ability of H_2O_2 oxidation to accurately mimic several aspects of biochar weathering in the field (Figure 1 and Table S1). In addition, we showed that the O/C ratio was correlated with three other relevant properties (DOC release, PFR concentration, ζ potential). Moreover, we found a negative correlation between O/C ratio and charcoal pH (Pearson $R = -0.8983$, $p = 0.0383$ excluding NH_2Cl aging), given that charcoal pH also plays a key role in the agricultural yield and soil microbiology (Figure S7). These correlations likely reflected the key role of surface oxidation in driving biochar environmental behaviors (both risks and benefits). However, PAH yield and contact angle did not correlate with the O/C ratio, which was also controlled by other factors (e.g., surface area and pore volume). Overall, this study provided evidence that it was possible to accurately predict biochar aging with a reduced suite of physicochemical properties. Future efforts can be put into exploring the generation of ROS (e.g., from UVA irradiation, activation of NH_2Cl,[68] or PFRs in contact with water, O_2, or H_2O_2) and its mechanism of action (e.g., char oxidation, release/degradation of DOC/PAHs) in the char aging systems.

Environmental Significance. There has been limited research on how the long-term biochar application affects the soil in the forest ecosystem.[113,114] Our decade-scale *in situ* field aging of wildfire-derived charcoal from the remains of the burned forest could be considered as a suitable proxy especially for application of woody biochar to forest soil.[6] However, there are differences in physicochemical properties between

https://doi.org/10.1021/acs.est.2c04751
Environ. Sci. Technol. 2023, 57, 128−138

anthropogenically and naturally produced charcoal (e.g., wildfire-derived charcoal tends to be more reactive and less stable than biochar).[115,116] Different feedstocks also lead to changes in biochar properties and their responses to aging (i.e., woody biomass could possess a lower ash and moisture content than animal/sludge-based biochar).[117] Additionally, we also recognize that other ecosystems, for instance, agricultural field sites, may have different soil types and/or microbial communities compared with the forest ecosystem. All of these aspects suggest that quantitative extrapolation of our findings should be conducted with care. However, some key aspects of our results can be extrapolated: char O/C ratio was well-correlated with changes in DOC release, PFR concentration, surface charge, and charcoal pH after aging.

Biochar field aging is a multilayered process, influenced by the presence of soil organic matter, minerals, microbes, and plant roots,[75] all of which add complexity to the system. Soil-forming factors are likely to play varying roles in charcoal aging. For example, freeze−thaw cycling will play a more important role in reducing particle size in colder regions.[7,118] However, the approaches reported here capture well the major alterations of char induced by long-term natural oxidation. This can be seen comparing the results reported here to those of Cheng et al.,[25] who reported changes in charcoal chemistry along a climosequence with a wide range in mean annual temperature (3.9−15.7 °C) and in mean annual precipitation (900−1370 mm). They also reported an increased O/C ratio, formation of surface oxygen functionalities, and evolution of surface negative charge.[25]

Overall, our study sheds light on the merits and limitations of accelerated aging to predict changes in biochar properties and its implications on associated ecosystem services. Our rapid, easily implemented, and verified lab-aging methods facilitate research toward derisking and enhancing long-term benefits of biochar application.

■ ASSOCIATED CONTENT

Supporting Information

The Supporting Information is available free of charge at https://pubs.acs.org/doi/10.1021/acs.est.2c04751.

Additional materials and methods details (Texts S1−S7); XPS survey and elemental scans (Figure S1); FTIR spectra (Figure S2); DOC release (Figure S3); explanation for DOC loss in the charcoal dark control experiment (Figure S4); EPR spectra, O/C vs PFR concentration, or ζ potential (Figure S5); HPLC chromatograms of PAHs (Figure S6); charcoal pH vs O/C (Figure S7); p value for simulation of field aging by lab aging (Table S1); XPS data (Table S2); textural data (Table S3); HPLC performance parameters (Table S4); and PAHs in charcoal (Table S5) (PDF)

■ AUTHOR INFORMATION

Corresponding Author

Caroline A. Masiello − *Department of Earth, Environmental and Planetary Sciences, Rice University, Houston, Texas 77005, United States; Carbon Hub, Rice University, Houston, Texas 77005, United States;* orcid.org/0000-0003-2102-6229; Phone: 713-348-5234; Email: masiello@rice.edu

Authors

Xiao Chen − *Department of Earth, Environmental and Planetary Sciences, Rice University, Houston, Texas 77005, United States; Carbon Hub, Rice University, Houston, Texas 77005, United States;* orcid.org/0000-0001-9129-9105

Xiaodong Gao − *Department of Earth, Environmental and Planetary Sciences, Rice University, Houston, Texas 77005, United States; Carbon Hub, Rice University, Houston, Texas 77005, United States*

Pingfeng Yu − *Department of Civil and Environmental Engineering, Rice University, Houston, Texas 77005, United States;* Present Address: College of Environmental and Resource Sciences, Zhejiang University, Hangzhou 310058, China; orcid.org/0000-0003-0402-773X

Leonardo Spanu − *Shell International Exploration & Production Inc., Houston, Texas 77082, United States*

Jessica Hinojosa − *Shell International Exploration & Production Inc., Houston, Texas 77082, United States*

Shuqi Zhang − *School of Environmental Science and Engineering, Key Laboratory of Thin Film and Microfabrication Technology (Ministry of Education), Shanghai Jiao Tong University, Shanghai 200240, China*

Mingce Long − *School of Environmental Science and Engineering, Key Laboratory of Thin Film and Microfabrication Technology (Ministry of Education), Shanghai Jiao Tong University, Shanghai 200240, China;* orcid.org/0000-0002-5168-8330

Pedro J. J. Alvarez − *Department of Civil and Environmental Engineering, Rice University, Houston, Texas 77005, United States;* orcid.org/0000-0002-6725-7199

Complete contact information is available at: https://pubs.acs.org/10.1021/acs.est.2c04751

Notes

The authors declare no competing financial interest.

■ ACKNOWLEDGMENTS

X.C., X.G., P.Y., P.J.J.A., and C.A.M. acknowledge financial support from Rice University's Carbon Hub, a nonprofit institute which receives corporate funding from Shell. M.L. and S.Z. acknowledge financial support from the National Natural Science Foundation of China (Nos. 52070128 and 21876108).

■ REFERENCES

(1) *Biochar for Environmental Management: Science and Technology*, 2nd ed.; Lehmann, J.; Joseph, S., Eds.; Earthscan: London, 2009.

(2) Woolf, D.; Amonette, J. E.; Street-Perrott, F. A.; Lehmann, J.; Joseph, S. Sustainable biochar to mitigate global climate change. *Nat. Commun.* **2010**, *1*, No. 56.

(3) Mathews, J. A. Carbon-negative biofuels. *Energy Policy* **2008**, *36*, 940−945.

(4) Renner, R. Rethinking biochar. *Environ. Sci. Technol.* **2007**, *41*, 5932−5933.

(5) Xie, T.; Reddy, K. R.; Wang, C.; Yargicoglu, E.; Spokas, K. Characteristics and applications of biochar for environmental remediation: A review. *Crit. Rev. Environ. Sci. Technol.* **2015**, *45*, 939−969.

(6) Mastrolonardo, G.; Calderaro, C.; Cocozza, C.; Hardy, B.; Dufey, J.; Cornelis, J. T. Long-term effect of charcoal accumulation in hearth soils on tree growth and nutrient cycling. *Front. Environ. Sci.* **2019**, *7*, No. 51.

(7) Wang, L.; O'Connor, D.; Rinklebe, J.; Ok, Y. S.; Tsang, D. C. W.; Shen, Z.; Hou, D. Biochar aging: Mechanisms, physicochemical

changes, assessment, and implications for field applications. *Environ. Sci. Technol.* **2020**, *54*, 14797−14814.
(8) Liu, Y.; Chen, J. Effect of ageing on biochar properties and pollutant management. *Chemosphere* **2022**, *292*, No. 133427.
(9) Qian, L.; Chen, B. Interactions of aluminum with biochars and oxidized biochars: Implications for the biochar aging process. *J. Agric. Food Chem.* **2014**, *62*, 373−380.
(10) Sanford, J. R.; Larson, R. A.; Runge, T. Nitrate sorption to biochar following chemical oxidation. *Sci. Total Environ.* **2019**, *669*, 938−947.
(11) Li, N.; Rao, F.; He, L.; Yang, S.; Bao, Y.; Huang, C.; Bao, M.; Chen, Y. Evaluation of biochar properties exposing to solar radiation: A promotion on surface activities. *Chem. Eng. J.* **2020**, *384*, No. 123353.
(12) Quan, G.; Fan, Q.; Cui, L.; Zimmerman, A. R.; Wang, H.; Zhu, Z.; Gao, B.; Wu, L.; Yan, J. Simulated photocatalytic aging of biochar in soil ecosystem: Insight into organic carbon release, surface physicochemical properties and cadmium sorption. *Environ. Res.* **2020**, *183*, No. 109241.
(13) Oleszczuk, P.; Kołtowski, M. Changes of total and freely dissolved polycyclic aromatic hydrocarbons and toxicity of biochars treated with various aging processes. *Environ. Pollut.* **2018**, *237*, 65−73.
(14) Hale, S.; Hanley, K.; Lehmann, J.; Zimmerman, A.; Cornelissen, G. Effects of chemical, biological, and physical aging as well as soil addition on the sorption of pyrene to activated carbon and biochar. *Environ. Sci. Technol.* **2011**, *45*, 10445−10453.
(15) Quan, G.; Fan, Q.; Zimmerman, A. R.; Sun, J.; Cui, L.; Wang, H.; Gao, B.; Yan, J. Effects of laboratory biotic aging on the characteristics of biochar and its water-soluble organic products. *J. Hazard. Mater.* **2020**, *382*, No. 121071.
(16) LeFevre, G. H.; Hozalski, R. M.; Novak, P. J. Root exudate enhanced contaminant desorption: An abiotic contribution to the rhizosphere effect. *Environ. Sci. Technol.* **2013**, *47*, 11545−11553.
(17) Yang, K.; Wang, X.; Cheng, H.; Tao, S. Effect of aging on stabilization of Cd and Ni by biochars and enzyme activities in a historically contaminated alkaline agricultural soil simulated with wet−dry and freeze−thaw cycling. *Environ. Pollut.* **2021**, *268*, No. 115846.
(18) Liu, B.; Liu, Q.; Wang, X.; Bei, Q.; Zhang, Y.; Lin, Z.; Liu, G.; Zhu, J.; Hu, T.; Jin, H.; Wang, H.; Sun, X.; Lin, X.; Xie, Z. A fast chemical oxidation method for predicting the long-term mineralization of biochar in soils. *Sci. Total Environ.* **2020**, *718*, No. 137390.
(19) Sigmund, G.; Bucheli, T. D.; Hilber, I.; Micić, V.; Kah, M.; Hofmann, T. Effect of ageing on the properties and polycyclic aromatic hydrocarbon composition of biochar. *Environ. Sci.: Processes Impacts* **2017**, *19*, 768−774.
(20) Erttmann, S. F.; Gekara, N. O. Hydrogen peroxide release by bacteria suppresses inflammasome-dependent innate immunity. *Nat. Commun.* **2019**, *10*, No. 3493.
(21) Veal, E. A.; Day, A. M.; Morgan, B. A. Hydrogen peroxide sensing and signaling. *Mol. Cell* **2007**, *26*, 1−14.
(22) Imlay, J. A. Cellular defenses against superoxide and hydrogen peroxide. *Annu. Rev. Biochem.* **2008**, *77*, 755−776.
(23) Farhat, N. M.; Loubineaud, E.; Prest, E.; El-Chakhtoura, J.; Salles, C.; Bucs, S. S.; Trampe, J.; Van den Broek, W. B. P.; Van Agtmaal, J. M. C.; Van Loosdrecht, M. C. M.; Kruithof, J. C.; Vrouwenvelder, J. S. Application of monochloramine for wastewater reuse: Effect on biostability during transport and biofouling in RO membranes. *J. Membr. Sci.* **2018**, *551*, 243−253.
(24) Askenaizer, D. Drinking Water Quality and Treatment. In *Encyclopedia of Physical Science and Technology*, 3rd ed.; Meyers, R. A., Ed.; Academic Press: New York, 2003; pp 651−671.
(25) Cheng, C.-H.; Lehmann, J.; Engelhard, M. H. Natural oxidation of black carbon in soils: Changes in molecular form and surface charge along a climosequence. *Geochim. Cosmochim. Acta* **2008**, *72*, 1598−1610.
(26) Briggs, C.; Breiner, J. M.; Graham, R. C. Physical and chemical properties of pinus ponderosa charcoal: Implications for soil modification. *Soil Sci.* **2012**, *177*, 263−268.
(27) Sigmund, G.; Santín, C.; Pignitter, M.; Tepe, N.; Doerr, S. H.; Hofmann, T. Environmentally persistent free radicals are ubiquitous in wildfire charcoals and remain stable for years. *Commun. Earth Environ.* **2021**, *2*, No. 68.
(28) Dittmar, T.; Paeng, J. A heat-induced molecular signature in marine dissolved organic matter. *Nat. Geosci.* **2009**, *2*, 175−179.
(29) Dittmar, T. The molecular level determination of black carbon in marine dissolved organic matter. *Org. Geochem.* **2008**, *39*, 396−407.
(30) Lalli, C. M.; Parsons, T. R. *Biological Oceanography: An Introduction*, 2nd ed.; Butterworth Heinemann: Oxford, 1997.
(31) Kiruri, L. W.; Khachatryan, L.; Dellinger, B.; Lomnicki, S. Effect of copper oxide concentration on the formation and persistency of environmentally persistent free radicals (EPFRs) in particulates. *Environ. Sci. Technol.* **2014**, *48*, 2212−2217.
(32) Lomnicki, S.; Truong, H.; Vejerano, E.; Dellinger, B. Copper oxide-based model of persistent free radical formation on combustion-derived particulate matter. *Environ. Sci. Technol.* **2008**, *42*, 4982−4988.
(33) Vejerano, E.; Lomnicki, S.; Dellinger, B. Formation and stabilization of combustion-generated environmentally persistent free radicals on an Fe(III)2O3/silica surface. *Environ. Sci. Technol.* **2011**, *45*, 589−594.
(34) Qiu, N.; Li, H.; Xu, E.; Qin, J.; Zheng, L. Temperature and time effects on free radical concentration in organic matter: Evidence from laboratory pyrolysis experimental and geological samples. *Energy Explor. Exploit.* **2012**, *30*, 311−329.
(35) Liao, S.; Pan, B.; Li, H.; Zhang, D.; Xing, B. Detecting free radicals in biochars and determining their ability to inhibit the germination and growth of corn, wheat and rice seedlings. *Environ. Sci. Technol.* **2014**, *48*, 8581−8587.
(36) Waggoner, D. C.; Wozniak, A. S.; Cory, R. M.; Hatcher, P. G. The role of reactive oxygen species in the degradation of lignin derived dissolved organic matter. *Geochim. Cosmochim. Acta* **2017**, *208*, 171−184.
(37) Mukherjee, A.; Zimmerman, A. R.; Harris, W. Surface chemistry variations among a series of laboratory-produced biochars. *Geoderma* **2011**, *163*, 247−255.
(38) Xu, R.; Wu, C.; Xu, H. Particle size and zeta potential of carbon black in liquid media. *Carbon* **2007**, *45*, 2806−2809.
(39) Letey, J.; Carrillo, M. L. K.; Pang, X. P. Approaches to characterize the degree of water repellency. *J. Hydrol.* **2000**, *231*−*232*, 61−65.
(40) Haleyur, N.; Shahsavari, E.; Mansur, A. A.; Koshlaf, E.; Morrison, P. D.; Osborn, A. M.; Ball, A. S. Comparison of rapid solvent extraction systems for the GC-MS/MS characterization of polycyclic aromatic hydrocarbons in aged, contaminated soil. *MethodsX* **2016**, *3*, 364−70.
(41) Perera, F. P. Environment and cancer: who are susceptible? *Science* **1997**, *278*, 1068−1073.
(42) Pyle, L. A.; Magee, K. L.; Gallagher, M. E.; Hockaday, W. C.; Masiello, C. A. Short-term changes in physical and chemical properties of soil charcoal support enhanced landscape mobility. *J. Geophys. Res.: Biogeosci.* **2017**, *122*, 3098−3107.
(43) Boehm, H. P. Carbon Surface Chemistry. In *Graphite and Precursors*; Delhaes, P., Ed.; Gordon and Breach Science Publishers: Amsterdam, 2001; pp 141−178.
(44) Cheng, C.-H.; Lehmann, J.; Thies, J. E.; Burton, S. D.; Engelhard, M. H. Oxidation of black carbon by biotic and abiotic processes. *Org. Geochem.* **2006**, *37*, 1477−1488.
(45) National Weather Service Website. https://www.weather.gov/hgx/climate_iah_normals_summary (accessed Sep 1, 2022).
(46) Liu, J.; Zhang, W. The Influence of the environment and clothing on human exposure to ultraviolet light. *PLoS One* **2015**, *10*, No. e0124758.
(47) Nishimura, K.; Ikehata, H.; Douki, T.; Cadet, J.; Sugiura, S.; Mori, T. Seasonal differences in the UVA/UVB ratio of natural

https://doi.org/10.1021/acs.est.2c04751
Environ. Sci. Technol. 2023, 57, 128−138

sunlight influence the efficiency of the photoisomerization of (6-4) photoproducts into their dewar valence isomers. *Photochem. Photobiol.* **2021**, *97*, 582−588.
(48) Corrêa, M. d. P. Solar ultraviolet radiation: properties, characteristics and amounts observed in Brazil and South America. *An. Bras. Dermatol.* **2015**, *90*, 297−310.
(49) Gouveia, G. R.; Trindade, G.; Nery, L.; Muelbert, J. UVA and UVB penetration in the water column of a south west atlantic warm temperate estuary and its effects on cells and fish larvae. *Estuaries Coasts* **2015**, *38*, 1147−1162.
(50) Qu, X.; Hwang, Y. S.; Alvarez, P. J. J.; Bouchard, D.; Li, Q. UV irradiation and humic acid mediate aggregation of aqueous fullerene (nC60) nanoparticles. *Environ. Sci. Technol.* **2010**, *44*, 7821−7826.
(51) Fu, H.; Liu, H.; Mao, J.; Chu, W.; Li, Q.; Alvarez, P. J. J.; Qu, X.; Zhu, D. Photochemistry of dissolved black carbon released from biochar: Reactive oxygen species generation and phototransformation. *Environ. Sci. Technol.* **2016**, *50*, 1218−1226.
(52) Yang, Y.; Javed, H.; Zhang, D.; Li, D.; Kamath, R.; McVey, K.; Sra, K.; Alvarez, P. Merits and limitations of TiO2-based photocatalytic pretreatment of soils impacted by crude oil for expediting bioremediation. *Front. Chem. Sci. Eng.* **2017**, *11*, 387−394.
(53) Chen, X.; Yang, L.; Myneni, S.; Deng, Y. Leaching of polycyclic aromatic hydrocarbons (PAHs) from sewage sludge-derived biochar. *Chem. Eng. J.* **2019**, *373*, 840−845.
(54) Matsunaka, T.; Nagao, S.; Inoue, M.; Mundo, R.; Tang, N.; Suzuki, N.; Ogiso, S.; Hayakawa, K. Temporal variations of polycyclic aromatic hydrocarbons in the seawater at tsukumo bay, Noto Peninsula, Japan, during 2014−2018. *Int. J. Environ. Res. Public Health* **2020**, *17*, No. 873.
(55) Kharbush, J. J.; Close, H. G.; Van Mooy, B. A. S.; Arnosti, C.; Smittenberg, R. H.; Le Moigne, F. A. C.; Mollenhauer, G.; Scholz-Böttcher, B.; Obreht, I.; Koch, B. P.; Becker, K. W.; Iversen, M. H.; Mohr, W. Particulate organic carbon deconstructed: Molecular and chemical composition of particulate organic carbon in the ocean. *Front. Mar. Sci.* **2020**, *7*, No. 518.
(56) Lawrinenko, M.; Laird, D.; Johnson, R.; Jing, D. Accelerated aging of biochars: Impact on anion exchange capacity. *Carbon* **2016**, *103*, 217−227.
(57) McLeod, J. W.; Gordon, J. Production of hydrogen peroxide by bacteria. *Biochem. J.* **1922**, *16*, 499−506.
(58) Whittenbury, R. Hydrogen peroxide formation and catalase activity in the lactic acid bacteria. *Microbiology* **1964**, *35*, 13−26.
(59) Hertzberger, R.; Arents, J.; Dekker, H. L.; Pridmore, R. D.; Gysler, C.; Kleerebezem, M.; de Mattos, M. J. T. H(2)O(2) production in species of the Lactobacillus acidophilus group: a central role for a novel NADH-dependent flavin reductase. *Appl. Environ. Microbiol.* **2014**, *80*, 2229−2239.
(60) Aller, D.; Rathke, S.; Laird, D.; Cruse, R.; Hatfield, J. Impacts of fresh and aged biochars on plant available water and water use efficiency. *Geoderma* **2017**, *307*, 114−121.
(61) Cross, A.; Sohi, S. P. A method for screening the relative long-term stability of biochar. *GCB Bioenergy* **2013**, *5*, 215−220.
(62) Jing, F.; Sohi, S. P.; Liu, Y.; Chen, J. Insight into mechanism of aged biochar for adsorption of PAEs: Reciprocal effects of ageing and coexisting Cd(2). *Environ. Pollut.* **2018**, *242*, 1098−1107.
(63) Luo, L.; Lv, J.; Chen, Z.; Huang, R.; Zhang, S. Insights into the attenuated sorption of organic compounds on black carbon aged in soil. *Environ. Pollut.* **2017**, *231*, 1469−1476.
(64) Mia, S.; Dijkstra, F. A.; Singh, B. Aging induced changes in biochar's functionality and adsorption behavior for phosphate and ammonium. *Environ. Sci. Technol.* **2017**, *51*, 8359−8367.
(65) Yang, F.; Zhao, L.; Gao, B.; Xu, X.; Cao, X. The interfacial behavior between biochar and soil minerals and its effect on biochar stability. *Environ. Sci. Technol.* **2016**, *50*, 2264−2271.
(66) Huff, M. D.; Lee, J. W. Biochar-surface oxygenation with hydrogen peroxide. *J. Environ. Manage.* **2016**, *165*, 17−21.
(67) Du, T.; Wang, Y.; Yang, X.; Wang, W.; Guo, H.; Xiong, X.; Gao, R.; Wuli, X.; Adeleye, A. S.; Li, Y. Mechanisms and kinetics study on the trihalomethanes formation with carbon nanoparticle precursors. *Chemosphere* **2016**, *154*, 391−397.
(68) Wang, Z.; Sun, P.; Li, Y.; Meng, T.; Li, Z.; Zhang, X.; Zhang, R.; Jia, H.; Yao, H. Reactive nitrogen species mediated degradation of estrogenic disrupting chemicals by biochar/monochloramine in buffered water and synthetic hydrolyzed urine. *Environ. Sci. Technol.* **2019**, *53*, 12688−12696.
(69) Roux, J. L.; Gallard, H.; Croué, J.-P.; Papot, S.; Deborde, M. NDMA formation by chloramination of ranitidine: Kinetics and mechanism. *Environ. Sci. Technol.* **2012**, *46*, 11095−11103.
(70) Zhang, M.; Wang, X.; Hao, H.; Wang, H.; Duan, L.; Li, Y. Formation of disinfection byproducts as affected by biochar during water treatment. *Chemosphere* **2019**, *233*, 190−197.
(71) Spokas, K. A.; Novak, J. M.; Masiello, C. A.; Johnson, M. G.; Colosky, E. C.; Ippolito, J. A.; Trigo, C. Physical disintegration of biochar: An overlooked process. *Environ. Sci. Technol. Lett.* **2014**, *1*, 326−332.
(72) Lehmann, J.; Liang, B.; Solomon, D.; Lerotic, M.; Luizão, F.; Kinyangi, J.; Schäfer, T.; Wirick, S.; Jacobsen, C. Near-edge X-ray absorption fine structure (NEXAFS) spectroscopy for mapping nano-scale distribution of organic carbon forms in soil: Application to black carbon particles. *Global Biogeochem. Cycles* **2005**, *19*, 1−12.
(73) Mukherjee, A.; Zimmerman, A. R. Organic carbon and nutrient release from a range of laboratory-produced biochars and biochar−soil mixtures. *Geoderma* **2013**, *193-194*, 122−130.
(74) Zimmerman, A. R. Abiotic and microbial oxidation of laboratory-produced black carbon (biochar). *Environ. Sci. Technol.* **2010**, *44*, 1295−1301.
(75) Joseph, S. D.; Camps-Arbestain, M.; Lin, Y.; Munroe, P.; Chia, C.; Hook, J.; Zwieten, L.; Kimber, S.; Cowie, A.; Singh, B.; Lehmann, J.; Foidl, N.; Smernik, R.; Amonette, J. An investigation into the reactions of biochar in soil. *Soil Res.* **2010**, *48*, 501−515.
(76) Sorrenti, G.; Masiello, C. A.; Dugan, B.; Toselli, M. Biochar physico-chemical properties as affected by environmental exposure. *Sci. Total Environ.* **2016**, *563-564*, 237−46.
(77) Boehm, H. P. Some aspects of the surface chemistry of carbon blacks and other carbons. *Carbon* **1994**, *32*, 759−769.
(78) Puri, B. R. Surfaces Complexes on Carbons. In *Chemistry and Physics of Carbon*; Walker, J. P. L., Ed.; Marcel Dekker: New York, 1970; pp 191−282.
(79) Hockaday, W. C.; Grannas, A. M.; Kim, S.; Hatcher, P. G. The transformation and mobility of charcoal in a fire-impacted watershed. *Geochim. Cosmochim. Acta* **2007**, *71*, 3432−3445.
(80) Kasozi, G. N.; Zimmerman, A. R.; Nkedi-Kizza, P.; Gao, B. Catechol and humic acid sorption onto a range of laboratory-produced black carbons (biochars). *Environ. Sci. Technol.* **2010**, *44*, 6189−6195.
(81) Castan, S.; Sigmund, G.; Hüffer, T.; Tepe, N.; von der Kammer, F.; Chefetz, B.; Hofmann, T. The importance of aromaticity to describe the interactions of organic matter with carbonaceous materials depends on molecular weight and sorbent geometry. *Environ. Sci.: Processes Impacts* **2020**, *22*, 1888−1897.
(82) Sigmund, G.; Arp, H. P. H.; Aumeier, B. M.; Bucheli, T. D.; Chefetz, B.; Chen, W.; Droge, S. T. J.; Endo, S.; Escher, B. I.; Hale, S. E.; Hofmann, T.; Pignatello, J.; Reemtsma, T.; Schmidt, T. C.; Schönsee, C. D.; Scheringer, M. Sorption and mobility of charged organic compounds: How to confront and overcome limitations in their assessment. *Environ. Sci. Technol.* **2022**, *56*, 4702−4710.
(83) Ding, Y.; Yamashita, Y.; Dodds, W. K.; Jaffe, R. Dissolved black carbon in grassland streams: Is there an effect of recent fire history? *Chemosphere* **2013**, *90*, 2557−2562.
(84) Dittmar, T.; de Rezende, C. E.; Manecki, M.; Niggemann, J.; Ovalle, A. R. C.; Stubbins, A.; Bernardes, M. C. Continuous flux of dissolved black carbon from a vanished tropical forest biome. *Nat. Geosci.* **2012**, *5*, 618−622.
(85) Abiven, S.; Hengartner, P.; Schneider, M. P. W.; Singh, N.; Schmidt, M. W. I. Pyrogenic carbon soluble fraction is larger and more aromatic in aged charcoal than in fresh charcoal. *Soil Biol. Biochem.* **2011**, *43*, 1615−1617.

https://doi.org/10.1021/acs.est.2c04751
Environ. Sci. Technol. 2023, 57, 128−138

(86) Wu, H.; Dong, X.; Liu, H. Evaluating fluorescent dissolved organic matter released from wetland-plant derived biochar: Effects of extracting solutions. *Chemosphere* **2018**, *212*, 638−644.
(87) Di Valentin, C.; Neyman, K. M.; Risse, T.; Sterrer, M.; Fischbach, E.; Freund, H.-J.; Nasluzov, V. A.; Pacchioni, G.; Rösch, N. Density-functional model cluster studies of EPR g tensors of Fs+ centers on the surface of MgO. *J. Chem. Phys.* **2006**, *124*, No. 044708.
(88) Hales, B. J.; Case, E. E. Immobilized radicals. IV. Biological semiquinone anions and neutral semiquinones. *Biochim. Biophys. Acta, Bioenerg.* **1981**, *637*, 291−302.
(89) Odinga, E. S.; Waigi, M. G.; Gudda, F. O.; Wang, J.; Yang, B.; Hu, X.; Li, S.; Gao, Y. Occurrence, formation, environmental fate and risks of environmentally persistent free radicals in biochars. *Environ. Int.* **2020**, *134*, No. 105172.
(90) Khachatryan, L.; Vejerano, E.; Lomnicki, S.; Dellinger, B. Environmentally persistent free radicals (EPFRs). 1. Generation of reactive oxygen species in aqueous solutions. *Environ. Sci. Technol.* **2011**, *45*, 8559−8566.
(91) Pignatello, J. J.; Mitch, W. A.; Xu, W. Activity and reactivity of pyrogenic carbonaceous matter toward organic compounds. *Environ. Sci. Technol.* **2017**, *51*, 8893−8908.
(92) Fang, G.; Gao, J.; Liu, C.; Dionysiou, D. D.; Wang, Y.; Zhou, D. Key role of persistent free radicals in hydrogen peroxide activation by biochar: Implications to organic contaminant degradation. *Environ. Sci. Technol.* **2014**, *48*, 1902−1910.
(93) Mia, S.; Dijkstra, F. A.; Singh, B. Long-Term Aging of Biochar: A Molecular Understanding with Agricultural and Environmental Implications. In *Advances in Agronomy*; Sparks, D. L., Ed.; Academic Press Inc.: Massachusetts, 2017; Vol. *141*, pp 1−51.
(94) Marcano-Martinez, E.; McBride, M. B. Comparison of the titration and ion adsorption methods for surface charge measurement in oxisols. *Soil Sci. Soc. Am. J.* **1989**, *53*, 1040−1045.
(95) Shi, K. S.; Xie, Y.; Qiu, Y. P. Natural oxidation of a temperature series of biochars: Opposite effect on the sorption of aromatic cationic herbicides. *Ecotoxicol. Environ. Saf.* **2015**, *114*, 102−108.
(96) Lehmann, J. Bio-energy in the black. *Front. Ecol. Environ.* **2007**, *5*, 381−387.
(97) Lehmann, J. A handful of carbon. *Nature* **2007**, *447*, 143−144.
(98) Wessel, A. T. On using the effective contact angle and the water drop penetration time for classification of water repellency in dune soils. *Earth Surf. Processes Landforms* **1988**, *13*, 555−561.
(99) Mao, J.; Zhang, K.; Chen, B. Linking hydrophobicity of biochar to the water repellency and water holding capacity of biochar-amended soil. *Environ. Pollut.* **2019**, *253*, 779−789.
(100) Wang, C.; Shang, C.; Ni, M. L.; Dai, J.; Jiang, F. (Photo)chlorination-induced physicochemical transformation of aqueous fullerene nC(60). *Environ. Sci. Technol.* **2012**, *46*, 9398−9405.
(101) Liu, Z.; Dugan, B.; Masiello, C. A.; Gonnermann, H. M. Biochar particle size, shape, and porosity act together to influence soil water properties. *PLoS One* **2017**, *12*, e0179079.
(102) Hilber, I.; Mayer, P.; Gouliarmou, V.; Hale, S. E.; Cornelissen, G.; Schmidt, H.-P.; Bucheli, T. D. Bioavailability and bioaccessibility of polycyclic aromatic hydrocarbons from (post-pyrolytically treated) biochars. *Chemosphere* **2017**, *174*, 700−707.
(103) European Biochar Certificate - Guidelines for a Sustainable Production of Biochar, Version 10.1 from 10th Jan 2022; European Biochar Foundation (EBC): Arbaz, Switzerland, 2012-2022. http://european-biochar.org.
(104) Khalid, F. N. M.; Klarup, D. The influence of sunlight and oxidative treatment on measured PAH concentrations in biochar. *Environ. Sci. Pollut. Res.* **2015**, *22*, 12975−12981.
(105) Hale, S. E.; Lehmann, J.; Rutherford, D.; Zimmerman, A. R.; Bachmann, R. T.; Shitumbanuma, V.; O'Toole, A.; Sundqvist, K. L.; Arp, H. P. H.; Cornelissen, G. Quantifying the total and bioavailable polycyclic aromatic hydrocarbons and dioxins in biochars. *Environ. Sci. Technol.* **2012**, *46*, 2830−2838.
(106) Bauschlicher Jr, C. W.; Ricca, A. Mechanisms for polycyclic aromatic hydrocarbon (PAH) growth. *Chem. Phys. Lett.* **2000**, *326*, 283−287.
(107) Radich, E. J.; Krenselewski, A. L.; Zhu, J.; Kamat, P. V. Is graphene a stable platform for photocatalysis? Mineralization of reduced graphene oxide with UV-irradiated TiO2 nanoparticles. *Chem. Mater.* **2014**, *26*, 4662−4668.
(108) Ricca, A.; Bauschlicher, C. W., Jr The reactions of polycyclic aromatic hydrocarbons with OH. *Chem. Phys. Lett.* **2000**, *328*, 396−402.
(109) Ukalska-Jaruga, A.; Debaene, G.; Smreczak, B. Dissipation and sorption processes of polycyclic aromatic hydrocarbons (PAHs) to organic matter in soils amended by exogenous rich-carbon material. *J. Soils Sediments* **2020**, *20*, 836−849.
(110) Pignatello, J. J. Interactions of Anthropogenic Organic Chemicals with Natural Organic Matter and Black Carbon in Environmental Particles. In *Biophysico-Chemical Processes of Anthropogenic Organic Compounds in Environmental Systems*; Wiley, 2011; pp 1−50.
(111) Ehlers, G. A. C.; Loibner, A. P. Linking organic pollutant (bio)availability with geosorbent properties and biomimetic methodology: A review of geosorbent characterisation and (bio)availability prediction. *Environ. Pollut.* **2006**, *141*, 494−512.
(112) Standardized Product Definition and Product Testing Guidelines for Biochar That is Used in Soil, Version 2.1, 23 November, document reference code: IBI-STD-2.1; Internatinal Biochar Initiative: Canandaigua, NY, 2015. https://biochar-international.org/wp-content/uploads/2020/06/IBI_Biochar_Standards_V2.1_Final2.pdf.
(113) Gundale, M. J.; Nilsson, M.-C.; Pluchon, N.; Wardle, D. A. The effect of biochar management on soil and plant community properties in a boreal forest. *GCB Bioenergy* **2016**, *8*, 777−789.
(114) Luo, Y.; Yu, Z.; Zhang, K.; Xu, J.; Brookes, P. C. The properties and functions of biochars in forest ecosystems. *J. Soils Sediments* **2016**, *16*, 2005−2020.
(115) Li, Y.; Hu, S.; Chen, J.; Müller, K.; Li, Y.; Fu, W.; Lin, Z.; Wang, H. Effects of biochar application in forest ecosystems on soil properties and greenhouse gas emissions: a review. *J. Soils Sediments* **2018**, *18*, 546−563.
(116) Santín, C.; Doerr, S. H.; Merino, A.; Bucheli, T. D.; Bryant, R.; Ascough, P.; Gao, X.; Masiello, C. A. Carbon sequestration potential and physicochemical properties differ between wildfire charcoals and slow-pyrolysis biochars. *Sci. Rep.* **2017**, *7*, No. 11233.
(117) Tomczyk, A.; Sokołowska, Z.; Boguta, P. Biochar physicochemical properties: pyrolysis temperature and feedstock kind effects. *Rev. Environ. Sci. Bio/Technol.* **2020**, *19*, 191−215.
(118) Li, H. X.; Lu, X. Q.; Xu, Y.; Liu, H. T. How close is artificial biochar aging to natural biochar aging in fields? A meta-analysis. *Geoderma* **2019**, *352*, 96−103.

https://doi.org/10.1021/acs.est.2c04751
Environ. Sci. Technol. 2023, 57, 128−138